Symmetry change of Co 3*d* orbital associated with the 500-K spin crossover accompanied by insulator-to-metal transition in $LaCoO_3$

Y. Kobayashi,[1,*] Y. Sakurai,[2] N. Tsuji,[2] K. Sato,[3] and K. Asai[4]

[1]*Department of Physics, Tokyo Medical University, Shinjuku, Tokyo 160-8402, Japan*

[2]*Japan Synchrotron Radiation Research Institute (JASRI), SPring-8, 1-1-1 Kouto, Sayo, Hyogo 679-5198, Japan*

[3]*Department of Industrial Engineering, National Institute of Technology, Ibaraki College, 866 Nakane, Hitachinaka Ibaraki 312-8508, Japan*

[4]*Department of Engineering Science, Graduate School of Informatics and Engineering, The University of Electro-Communications, Chofu, Tokyo 182-8585, Japan*

(Received 26 June 2018; revised manuscript received 9 August 2018; published 26 September 2018)

We have carried out the imaging of the electron momentum density of Co 3*d* electrons in $LaCoO_3$ using x-ray Compton scattering, in order to investigate the electron-orbital states relevant to the spin-crossover phenomenon at around 500 K, where an insulator-metal transition takes place. The electron momentum density reconstructed from the Compton profiles indicates the symmetry change in the Co 3*d* electron-orbital states between below and above 500 K, which reveals the electron transfer from t_{2g} to e_g orbitals similar to that of the spin crossover around 100 K. The magnitude of the anisotropy change in the Compton profiles exhibits a steep increase at around 500 K, implying a cooperative characteristics of the 500-K spin-crossover phenomenon. The Compton profiles also show an increment of the molecular orbital feature by the development of the hybridization between Co 3*d* and O 2*p* orbitals with increasing temperature.

DOI: 10.1103/PhysRevB.98.115154

I. INTRODUCTION

Trivalent cobalt oxides have attracted interest because of their diverse properties, which are attributed to the multiple degrees of freedom on spin, orbital, and lattice associated with $3d^6$ electronic configuration of Co^{3+}. One of the typical examples is the spin-crossover phenomena in Perovskite cobaltite $RECoO_3$ (RE: rare-earth elements or Y). $RECoO_3$ exhibits a broad magnetic anomaly at around 500–700 K. It has been reported that Co^{3+} ions in $RECoO_3$ change its spin state from a nonmagnetic low-spin (LS: $^1A_1, t_{2g}^6 e_g^0, S = 0$) ground state to a magnetic excited state [1–8]. The spin-state change is accompanied by an insulator-to-metal (I-M) transition where the resistivity ρ shows a significant decrease, and exhibits a metal-like temperature dependence above 500–700 K [7,9]. $LaCoO_3$ has been considered to show another spin-crossover phenomenon at around 100 K in addition to that at around 500 K [3,10,11]. The most controversial issue regarding the spin-crossover phenomenon in $LaCoO_3$ is the spin states of Co 3*d* in the magnetic excited state involved in the 100-K spin crossover. Based on the ligand-field theory, most likely excited state for Co^{3+} is the high-spin (HS: $^5T_2, t_{2g}^4 e_g^2, S = 2$) state, and the intermediate spin (IS: $^3T_1, t_{2g}^5 e_g^1, S = 1$) state is possible [12]. In spite of the extensive amounts of research, it has not been concluded yet whether the first magnetic excited state is HS or IS state [13–35].

As described above, the spin-crossover phenomena in $RECoO_3$ cannot be simply understood by the ligand-field theory in contrast to the spin crossover in most other transition-metal compounds and complexes. One of the reasons for the difficulty in understanding the anomalous spin-crossover phenomena in $RECoO_3$ is the collective nature arising from the interactions among 3*d* electrons on the neighboring Co^{3+}, which is larger than or equivalent to the energy difference between the LS and the magnetic excited states of a single ion [25]. This means that the spin-crossover phenomena in $RECoO_3$ should not be understood by the ligand-field theory of the single CoO_6 octahedra, and should be treated with considerations taking into account the correlation among the Co 3*d* electronic-orbital states. Recently, calculations on the basis of dynamical mean-field theory such as *dp* model simulation of Co 3*d* and O 2*p* orbitals [36] and proposals of excitonic-insulating phase as a quantum mixed state between LS and HS states [37–39] have been reported. Therefore, detailed experimental researches on the electron-orbital states of Co 3*d* responsible for the spin crossover are indispensable for understanding the spin-crossover phenomena in $RECoO_3$.

In order to investigate the Co 3*d* electron-orbital states, such as the symmetry and distribution of the 3*d*-electron orbital states in $LaCoO_3$, we have conducted x-ray Compton scattering experiments. The x-ray Compton scattering experiments enable the imaging of the electron density distribution in the momentum space [40–44]. The Compton profiles $J(p_z)$ reflect the projection of the three-dimensional electron momentum density $\rho(p_x, p_y, p_z)$ onto the z axis, which lies along the scattering vector

$$J(p_z) = \iint \rho(p_x, p_y, p_z) dp_x dp_y. \quad (1)$$

The electron momentum density can be reconstructed using the Compton profiles measured along the several crystallographic directions. Using the Compton profiles measured

*koba@tokyo-med.ac.jp

below and above the spin crossover, we can obtain the reconstructed electron momentum density which exhibits the Co $3d$ electron-orbital states responsible for the spin-crossover phenomena in $LaCoO_3$ [45]. We have obtained the results below 300 K [45] as (i) an orbital symmetry change demonstrating the electron transfer from t_{2g} to e_g orbitals through the 100-K spin crossover, and (ii) the feature of the molecular orbitals both below and above the spin crossover resulting from the Co($3d$)-O($2p$) hybridization in Co $3d$ states, which has been argued previously [17,18,28,46].

In this paper we report the results of the x-ray Compton scattering experiments on $LaCoO_3$ below and above 500 K. The previous reports of the magnetic susceptibility and the ^{59}Co Knight shift of $RECoO_3$ exhibits broad steplike anomalies at around 500–700 K, where the I-M transition takes place [5–7,16]. These facts suggest a significant change in the electron-spin states of Co^{3+} at around 500–700 K in $RECoO_3$, although few researches on the electronic state associated with this spin-crossover phenomena in perovskite cobaltites have been reported. Thus we have investigated the electron momentum density of the Co $3d$ states in $LaCoO_3$ in order to evaluate the characteristics of the electron-orbital states responsible for the spin-crossover phenomenon accompanied by the I-M transition at around 500 K.

II. EXPERIMENTAL PROCEDURE

Single crystals of $LaCoO_3$ were grown using a lamp-image floating zone furnace by melting polycrystalline samples prepared by a solid-state reaction of predried La_2O_3 and CoO. The single crystals were confirmed to be of a single phase by x-ray powder diffraction after being ground. In this paper we use the crystallographic indices $[hkl]_c$ based on the pseudocubic primitive unit cell containing one chemical formula of $LaCoO_3$, since the rhombohedral distortion of the crystal from the cubic symmetry is small and the crystals have a twinned structure.

The Compton scattering experiments were conducted using the beamline BL08W at SPring-8, Japan. The resolution of the measured Compton profiles is about 0.6 atomic units (a.u.) in the momentum space. The Compton profiles were measured at 303 and 573 K in six directions equally spaced (9°) between the $[100]_c$ and $[110]_c$ axes of the pseudocubic cell. The measured Compton profile intensity was normalized by the total electron number of $LaCoO_3$. Then the difference of the Compton profiles between 303 and 573 K was obtained for each direction. The difference of the two-dimensional electron momentum density (2D-EMD) of Co $3d$ projected in the $[001]_c$ direction was reconstructed using the difference Compton profiles [40]. We also measured the Compton profiles along $[100]_c$ direction at several temperatures between 303 and 663 K in order to obtain the detailed temperature dependence of the Compton profiles.

In order to evaluate the measured Compton profiles and the reconstructed difference 2D-EMD, we performed a molecular orbital (MO) calculation taking into account the hybridization between Co $3d$ and O $2p$. The MO calculation was conducted by the molecular orbital as a linear combination of atomic orbitals (LCAO-MO) method in which MO was obtained by adding atomic orbitals of $2p$ and/or $2s$ states on ligand O ions to atomic Co e_g ($3z^2 - r^2$ and $x^2 - y^2$) and/or Co t_{2g} (xy, yz, and zx) states in the same manner as reported in Ref. [47] assuming a cubic symmetry. The three covalency parameters f_π, f_σ, and f_s are set to be 0.10, 0.20, and 0.04, respectively, which are close to those for Fe_3O_4 described in Ref. [47].

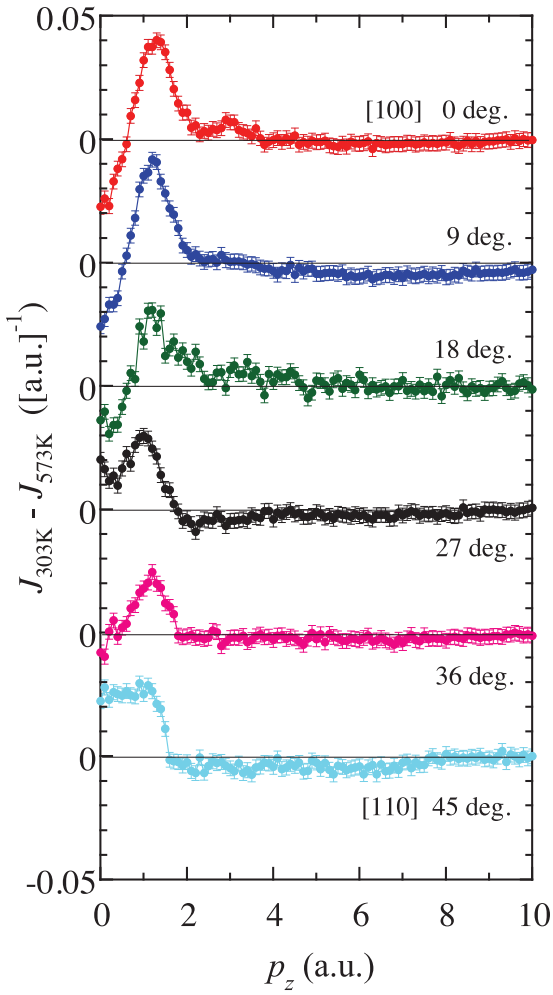

FIG. 1. Difference Compton profiles ($J_{303\,K} - J_{573\,K}$) for six directions between $[100]_c$ and $[110]_c$ in $LaCoO_3$.

III. EXPERIMENTAL RESULTS

Figure 1 shows the difference Compton profiles ($J_{303\,K} - J_{573\,K}$) in six directions between $[100]_c$ and $[110]_c$ in $LaCoO_3$. The difference Compton profiles between 303 and 573 K with a significant magnitude for each direction strongly indicate the symmetry change of the electron momentum density through the spin crossover at around 500 K. The shape and magnitude of the difference Compton profiles for each crystalline direction are similar to those ($J_{10\,K} - J_{270\,K}$) obtained for the spin crossover at around 100 K shown in Fig. 1 of Ref. [45]. Thus these results of the Compton profile measurements indicate that the symmetry change of Co $3d$ orbitals similar to that associated with the 100-K spin crossover also takes place between 303 and 573 K in $LaCoO_3$.

The difference 2D-EMD was reconstructed from the difference Compton profiles as shown in Fig. 2. The experimentally

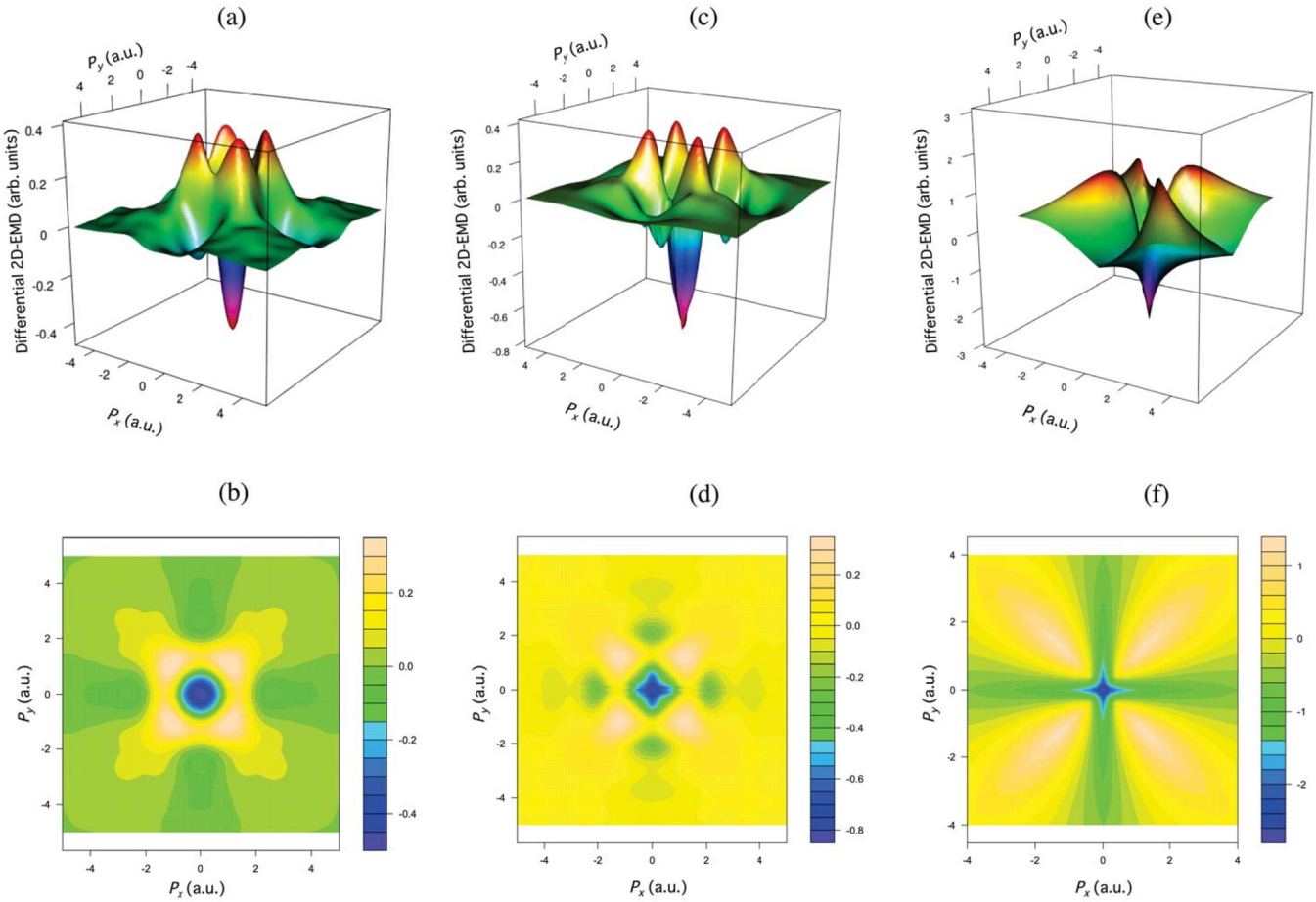

FIG. 2. (a) The aerial view and (b) contour plot of the difference two-dimensional electron momentum density (2D-EMD) of Co 3*d* projected along $[001]_c$ reconstructed using the difference Compton profiles shown in Fig. 1, along with those of the calculated molecular [(c) and (d)] and atomic orbitals [(e) and (f)] [45].

obtained difference 2D-EMD [see Figs. 2(a) and 2(b)] shows a positive component of the electron density extending toward $\langle 110\rangle_c$, whereas a negative component extending toward $\langle 100\rangle_c$. These findings can be explained by the electron transfer from t_{2g} (xy, yz, and zx) to e_g ($3z^2 - r^2$ and $x^2 - y^2$) orbitals with increasing temperature, which has already been reported for the 100-K spin crossover in $LaCoO_3$ [45]. Thus the difference 2D-EMD provides direct evidence for the electron transfer from t_{2g} to e_g orbitals associated with the 500-K spin crossover in $LaCoO_3$ [45].

As shown in the reconstructed difference 2D-EMD [see Figs. 2(a) and 2(b)], the region with the large magnitude is localized in the region where p_x and p_y are less than ∼2 a.u. This characteristic is in agreement with that for the calculated difference 2D-EMD of MO taking into account the Co(3*d*)-O(2*p*) hybridization [see Figs. 2(c) and 2(d)] and different from that of the atomic orbitals for localized 3*d* electrons [see Figs. 2(e) and 2(f)] [48]. This finding indicates the MO feature of the electron-orbital state relevant to the 500-K spin-crossover phenomena in $LaCoO_3$, which results from covalent bonding between Co 3*d* and O 2*p* orbitals [17,18,28,46].

In order to clarify the temperature dependence of the symmetry change of Co 3*d* between 303 and 573 K, we measured the difference Compton profiles in the $[100]_c$ direction with changing temperature. The difference Compton profiles between 303 K and the measured temperature ($J_{303\,\mathrm{K}} - J_T$) are shown in Fig. 3(a). The shape of the difference Compton profiles is almost unchanged with changing temperature, although its magnitude increases remarkably with increasing temperature. These findings imply that the electron transfer from t_{2g} to e_g orbitals maintains at higher temperatures.

The shape of the difference Compton profile suggests also the enhancement of the molecular orbital formation with increasing temperature. We have already reported that the difference Compton profile for the 100-K spin crossover ($J_{10\,\mathrm{K}} - J_{270\,\mathrm{K}}$) shows an oscillation at approximately $p_z =$ 2–4 a.u. [45], which is the characteristic of the molecular orbitals constructed by hybridization between Co e_g and O 2*p* orbitals [41–43]. Indeed, the oscillation is reproduced in the difference Compton profiles calculated for the MO, whereas it does not appear for localized atomic orbitals, as shown in Fig. 3(b). The oscillatory behavior in the difference Compton profile becomes prominent for higher temperatures as shown in Fig. 3. In order to evaluate the hybridization effect between Co e_g and O 2*p* orbitals with changing temperature, we plotted the temperature dependence of the ratio of the oscillation amplitude (A_O) to the total amplitude (A_T) of the difference Compton profiles for each temperature including the results of the previous study [45] as shown in Fig. 4. Note that we added the amplitudes A_O and A_T at 270 K

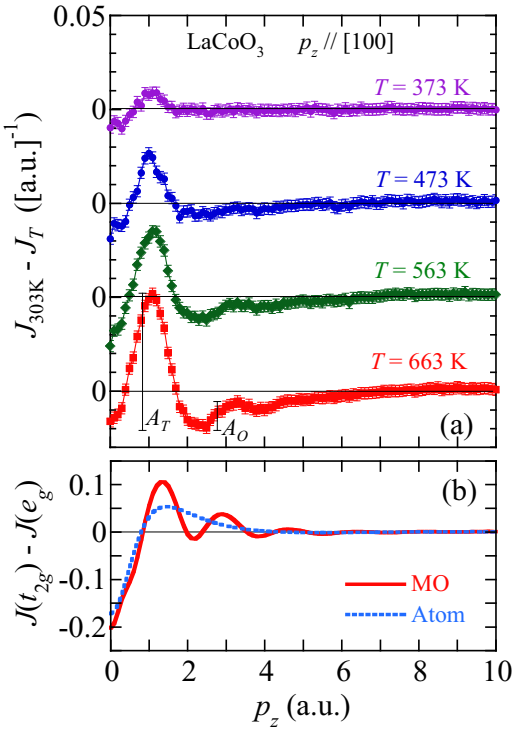

FIG. 3. (a) Temperature dependence of the difference Compton profiles ($J_{303\,\mathrm{K}} - J_T$) for $[100]_c$ direction, along with (b) the calculated difference Compton profiles for molecular orbitals (MO) and localized atomic orbitals (Atom). The oscillation amplitude (A_O) and the total amplitude (A_T) for $T = 663$ K are also shown.

obtained from the difference Compton profile ($J_{10\,\mathrm{K}} - J_{270\,\mathrm{K}}$) [45] to those above 300 K shown in Fig. 3 to standardize the reference temperature to 10 K. (The difference between $J_{270\,\mathrm{K}}$ and $J_{303\,\mathrm{K}}$ is small enough to be neglected.) The ratio increases with increasing temperature, which strongly suggests the development of the molecular orbital formation resulting from the increment of the hybridization between Co e_g and O $2p$ orbitals.

Figure 5 shows the temperature dependence of the area intensity of the difference Compton profile $I_{\Delta J}$

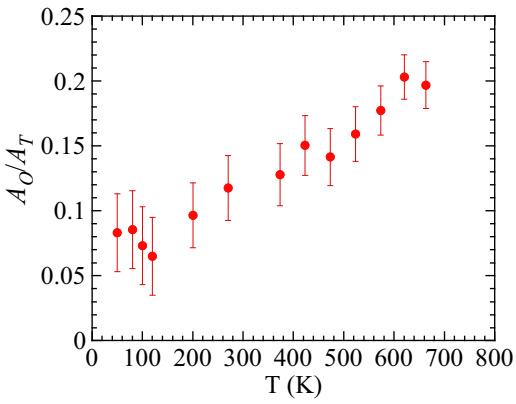

FIG. 4. Temperature dependence of the ratio of the oscillation amplitude to the total amplitude (A_O/A_T) of the difference Compton profiles for $[100]_c$ direction.

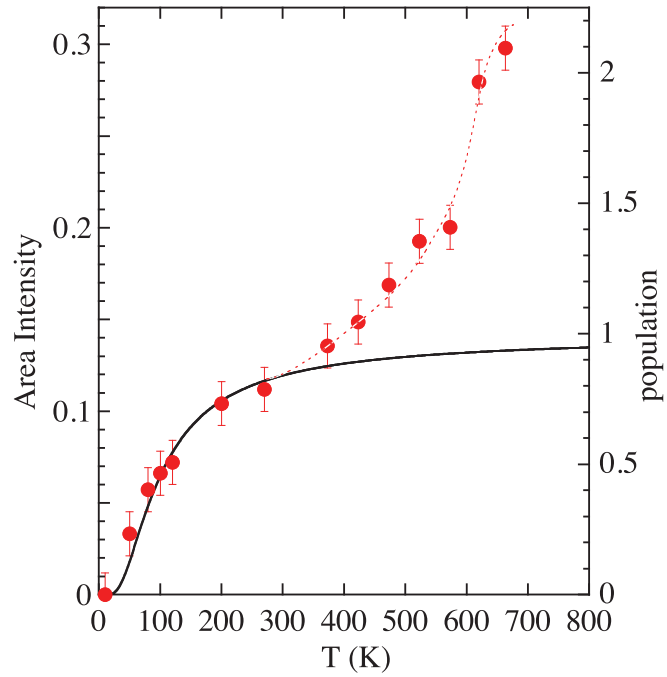

FIG. 5. Temperature dependence of the area intensity of difference Compton profile $I_{\Delta J}$ ($= \int_0^{10} |J_{10\,\mathrm{K}} - J_T| dp_z$) along $[100]_c$ direction. The dotted line is the guide for eyes. The solid line shows the population of the magnetic Co species calculated according to the thermal excitation model [35].

($= \int_0^{10} |J_{10\,\mathrm{K}} - J_T| dp_z$) along $[100]_c$ direction, including the previous results between 10 and 270 K [45]. The area intensity $I_{\Delta J}$ between 303 and 663 K shown in Fig. 5 was obtained by adding the value of $I_{\Delta J}$ at 303 K to $\int_0^{10} |J_{303\,\mathrm{K}} - J_T| dp_z$, in which $I_{\Delta J}$ at 303 K was derived from the extrapolation of the previous result of $I_{\Delta J}(T)$ between 10 and 270 K [45]. $I_{\Delta J}(T)$ exhibits a significant increase above about 400 K, and shows a tendency to saturate above 600 K, which implies a presence of an electronic transition. The temperature dependence of $I_{\Delta J}$ is similar to that of the total amplitude of the difference Compton profiles (A_T) (not shown). The steplike increment of $I_{\Delta J}$ is different from the monotonous temperature dependence of the population of HS shown in Fig. 3(a) of Ref. [28]. Temperature dependence of the total population of the magnetic Co species (HS and IS) calculated according to the thermal excitation model [35] is also shown in Fig. 5. The deviation of the measured $I_{\Delta J}(T)$ above about 400 K from the calculated population is remarkable, in contrast to that of $I_{\Delta J}(T)$ between 10 and 270 K (see Fig. 5). This finding implies the cooperative nature of the electron transfer associated with the spin crossover at around 500 K, in contrast to the 100-K spin crossover exhibiting the thermal excitation type temperature dependence.

IV. DISCUSSION

A. The shape of the Compton profiles

The difference Compton profiles and the reconstructed difference 2D-EMD between 303 and 573 K (see Figs. 1 and 2) reveal the symmetry change of the Co $3d$ electron-orbital state

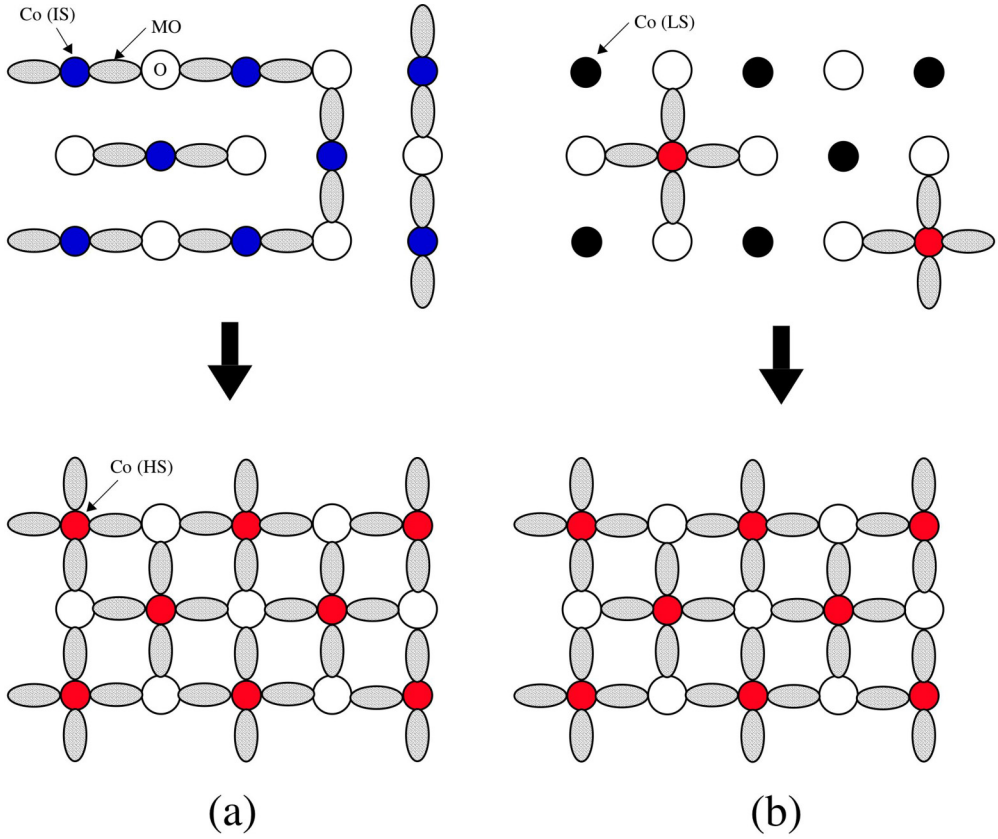

FIG. 6. Schematic figures showing the development of Co(3*d*)-O(2*p*) hybridization and the MO formation at higher temperatures. (a) The difference of the contribution to the hybridization between the spin states of Co^{3+} and (b) a percolation of magnetic Co species.

above 500 K. The shape and the magnitude of the difference Compton profiles and difference 2D-EMD are similar to those for the 100-K spin crossover [45]. The findings suggest that the t_{2g}-e_g electron transfer responsible for the spin-crossover phenomena significantly enhances above 500 K.

The oscillatory behavior in the difference Compton profiles between $p_z = \sim$ 2–4 a.u. becomes remarkable for higher temperatures as shown in Fig. 3. The oscillation amplitude shows a significant increase with increasing temperature (see Fig. 4), although a steep increment at around 500 K similar to $I_{\Delta J}(T)$ is not apparent. These findings exhibit a development of the MO formation resulting from the progress of the hybridization effect between Co e_g and O 2*p* orbitals through the spin-crossover phenomena. The development of the MO formation implies the collectiveness of the spin-crossover phenomena in $LaCoO_3$, since the nonlocal electron-orbital state plays an important role on the spin crossover.

As the origin of the development of Co(3*d*)-O(2*p*) hybridization and the MO formation at higher temperatures, two possible scenarios can be considered. The first one is the difference of the hybridization due to the different spin states of Co^{3+}. The IS state has one electron in e_g orbital which extends to O 2*p* orbital, whereas the HS state has two electrons. Thus it seems natural that the MO formation due to the Co(e_g)-O(2*p*) bonding proceeds more for HS state than IS state. If one electron transfers at around 100 K and another one at around 500 K, the more developed MO character after 500-K transition can be expected [see Fig. 6(a)]. This picture is compatible with LS-IS-HS two-stage spin-state transition model [16]. The second is a percolation of magnetic Co species, where HS (or IS) Co are excited in LS Co matrix with increasing temperature. At comparatively low temperature where the number of the magnetic Co ions with e_g electrons is small, each cluster connected by the Co(3*d*)-O(2*p*) hybridization between adjacent Co^{3+} and O^{2-} ions is limited within a narrow area. With increasing the number of the magnetic Co at higher temperature, the network of the Co(3*d*)-O(2*p*)-Co(3*d*) bondings spread over the crystal and consequently the MO formation develops [see Fig. 6(b)]. The development of the MO character above 300 K can be interpreted as the percolation develops at temperatures higher than 300 K based on the model. Thus this picture seems to be compatible with LS-HS model. Since both scenarios can explain the results of the present experiment, we cannot determine whether the HS or IS is the spin state at higher temperatures. Therefore, the precise analysis of the MO is indispensable in order to determine which perspective is more adequate.

B. The area intensity of the Compton profiles

The temperature dependence of the area intensity of the difference Compton profile $I_{\Delta J}$ shows a steep increase at around 500 K, in contrast to the thermal-activation-like increment below 300 K (see Fig. 5), which suggests the cooperative character of the 500-K spin crossover as described above. The development of the Co(3*d*)-O(2*p*) hybridization and the MO formation throughout the crystal above 500 K might produce the cooperative character of the 500-K spin crossover; i.e., the

I-M transition through the development of the MO formation might produce the cooperative character of the 500-K spin crossover.

The magnitude of the increment of $I_{\Delta J}$ at around 500 K is close to that between 0 and 300 K as shown in Fig. 5. The fact indicates that the magnitude of the electron transfer for the 500-K spin crossover is comparable with that for 100-K spin crossover. This inference is supported by the anomalous thermal lattice expansion of $LaCoO_3$, in which the magnitude of the lattice expansion for the 500-K spin crossover is almost equivalent to that for the 100-K spin crossover [16]. On the other hand, temperature dependence of the effective magnetic moment ($p_{\rm eff}$) estimated from the magnetization measurements shows that the increase of $p_{\rm eff}$ around 500 K is much smaller than that between 0 and 300 K [16]. The apparent contradiction between the present Compton scattering experiments and the magnetization measurements suggests that the magnetic moment induced by the 500-K spin crossover is much smaller than that induced by the 100-K spin crossover, despite that the magnitude of the electron transfer between t_{2g} and e_g orbitals is comparable between 100- and 500-K spin-crossover phenomena. This finding implies that the electron-orbital state induced by the 500-K spin crossover has a different magnitude of the magnetic moment from that induced by the 100-K spin crossover. If HS Co^{3+} with $S = 2$ is induced owing to the 500-K spin crossover, larger magnetization is expected to be observed above 500 K. We infer that the MO formation resulting from the Co($3d$)-O($2p$) hybridization is responsible for the smallness of $p_{\rm eff}$. $p_{\rm eff}$ is expected to be different if the electron-orbital state is largely different from the ionic Co $3d$.

In order to discuss the $p_{\rm eff}$ on the 500-K spin crossover, previous investigations on the magnetization in Sr-doped $LaCoO_3$ would be helpful. Okamoto *et al.* have investigated the magnetic moment of Co in $La_{1-x}Sr_xCoO_3$ using the magnetic circular x-ray dichroism (MCXD) and magnetization measurements [49]. The magnitude of the averaged magnetization for the ferromagnetic metallic phase of $La_{1-x}Sr_xCoO_3$ ($x \gtrsim 0.4$) is less than 2 μ_B/Co. This value seems to be too small for the magnetic moment of HS Co^{3+} with $S = 2$, even taking into account the coexistence of Co^{4+} moment in $La_{1-x}Sr_xCoO_3$ owing to the Sr^{2+} doping. In the report they attributed the smallness of the magnetic moment to the itineracy of the Co $3d$ electrons [49]. Their supposition supports our consideration that the development of the MO formation above 500 K is associated with the smallness of the $p_{\rm eff}$.

V. CONCLUSION

The electron momentum density reconstructed from the Compton profiles indicates the symmetry change in the $3d$ electron-orbital states between below and above 500 K, which reveals that the electron transfer from t_{2g} to e_g orbitals arises also at around 500 K in $LaCoO_3$. The magnitude of the difference Compton profiles exhibits a steep increase at around 500 K, implying a cooperative character of the 500-K spin-crossover phenomenon. The difference Compton profiles show an increment of the characteristics of hybridization between Co $3d$ and O $2p$ orbitals, which suggests the development of the molecular orbital formation.

ACKNOWLEDGMENTS

The authors thank Dr. M. Itou for his experimental assistance. The synchrotron radiation experiments were performed with the approval of the Japan Synchrotron Radiation Research Institute (JASRI), SPring-8 (Proposals No. 2011B1298, No. 2012A1714, No. 2013A1023, No. 2014B1201, No. 2015A1211, No. 2016B1067, and No. 2017A1175).

[1] J. B. Goodenough, J. Phys. Chem. Solids **6**, 287 (1958).
[2] J. B. Goodenough and J. M. Longo, *Landolt-Börnstein* (Springer, Berlin, 1970), Vol. 4a, Chap. 3.
[3] R. R. Heikes, R. C. Miller, and R. Mazelsky, Physica **30**, 1600 (1964).
[4] G. Thornton, F. C. Morrison, S. Partington, B. C. Tofield, and D. E. Williams, J. Phys. C **21**, 2871 (1988).
[5] M. Itoh, M. Mori, S. Yamaguchi, and Y. Tokura, Physica B (Amsterdam) **259-261**, 902 (1999).
[6] M. Itoh, J. Hashimoto, S. Yamaguchi, and Y. Tokura, Physica B (Amsterdam) **281-282**, 510 (2000).
[7] S. Yamaguchi, Y. Okimoto, and Y. Tokura, Phys. Rev. B **54**, R11022 (1996).
[8] K. Knizek, Z. Jirak, J. Hejtmanek, M. Veverka, M. Marysko, B. C. Hauback, and H. Fjellvag, Phys. Rev. B **73**, 214443 (2006).
[9] Y. Kobayashi, S. Murata, K. Asai, J. M. Tranquada, G. Shirane, and K. Kohn, J. Phys. Soc. Jpn. **69**, 3468 (2000).
[10] G. H. Jonker, J. Appl. Phys. **37**, 1424 (1966).
[11] P. M. Raccah and J. B. Goodenough, Phys. Rev. **155**, 932 (1967).
[12] Y. Tanabe and S. Sugano, J. Phys. Soc. Jpn. **9**, 766 (1954).
[13] K. Asai, P. Gehring, H. Chou, and G. Shirane, Phys. Rev. B **40**, 10982 (1989).
[14] K. Asai, O. Yokokura, N. Nishimori, H. Chou, J. M. Tranquada, G. Shirane, S. Higuchi, Y. Okajima, and K. Kohn, Phys. Rev. B **50**, 3025 (1994).
[15] K. Asai, O. Yokokura, M. Suzuki, T. Naka, T. Matsumoto, H. Takahashi, N. Mori, and K. Kohn, J. Phys. Soc. Jpn. **66**, 967 (1997).
[16] K. Asai, A. Yoneda, O. Yokokura, J. M. Tranquada, G. Shirane, and K. Kohn, J. Phys. Soc. Jpn. **67**, 290 (1998).
[17] M. A. Korotin, S. Y. Ezhov, I. V. Solovyev, V. I. Anisimov, D. I. Khomskii, and G. A. Sawatzky, Phys. Rev. B **54**, 5309 (1996).
[18] T. Saitoh, T. Mizokawa, A. Fujimori, M. Abbate, Y. Takeda, and M. Takano, Phys. Rev. B **55**, 4257 (1997).

[19] Y. Kobayashi, N. Fujiwara, S. Murata, K. Asai, and H. Yasuoka, Phys. Rev. B **62**, 410 (2000).
[20] G. Maris, Y. Ren, V. Volotchaev, C. Zobel, T. Lorenz, and T. T. M. Palstra, Phys. Rev. B **67**, 224423 (2003).
[21] A. Ishikawa, J. Nohara, and S. Sugai, Phys. Rev. Lett. **93**, 136401 (2004).
[22] Y. Kobayashi, T. S. Naing, M. Suzuki, M. Akimitsu, K. Asai, K. Yamada, J. Akimitsu, P. Manuel, J. M. Tranquada, and G. Shirane, Phys. Rev. B **72**, 174405 (2005).
[23] T. S. Naing, T. Kobayashi, Y. Kobayashi, M. Suzuki, and K. Asai, J. Phys. Soc. Jpn. **75**, 084601 (2006).
[24] S. Noguchi, S. Kawamata, K. Okuda, H. Nojiri, and M. Motokawa, Phys. Rev. B **66**, 094404 (2002).
[25] T. Kyomen, Y. Asaka, and M. Itoh, Phys. Rev. B **71**, 024418 (2005).
[26] W. Low and M. Weger, Phys. Rev. **118**, 1119 (1960).
[27] W. Low and M. Weger, Phys. Rev. **118**, 1130 (1960).
[28] M. W. Haverkort, Z. Hu, J. C. Cezar, T. Burnus, H. Hartmann, M. Reuther, C. Zobel, T. Lorenz, A. Tanaka, N. B. Brookes, H. H. Hsieh, H.-J. Lin, C. T. Chen, and L. H. Tjeng, Phys. Rev. Lett. **97**, 176405 (2006).
[29] K. Knizek, J. Hejtmanek, M. Marysko, Z. Jirak, and J. Bursik, Phys. Rev. B **85**, 134401 (2012).
[30] Y. Shimizu, T. Takahashi, S. Yamada, A. Shimokata, T. Jin-no, and M. Itoh, Phys. Rev. Lett. **119**, 267203 (2017).
[31] K. Tomiyasu, J. Okamoto, H. Y. Huang, Z. Y. Chen, E. P. Sinaga, W. B. Wu, Y. Y. Chu, A. Singh, R.-P. Wang, F. M. F. de Groot, A. Chainani, S. Ishihara, C. T. Chen, and D. J. Huang, Phys. Rev. Lett. **119**, 196402 (2017).
[32] K. Sato, M. I. Bartashevich, T. Goto, Y. Kobayashi, M. Suzuki, K. Asai, A. Matsuo, and K. Kindo, J. Phys. Soc. Jpn. **77**, 024601 (2008).
[33] K. Sato, A. Matsuo, K. Kindo, Y. Kobayashi, and K. Asai, J. Phys. Soc. Jpn. **78**, 093702 (2009).
[34] K. Sato, A. Matsuo, K. Kindo, Y. Kobayashi, and K. Asai, J. Phys. Soc. Jpn. **80**, 104702 (2011).
[35] K. Sato, A. Matsuo, K. Kindo, Y. Hara, K. Nakaoka, Y. Kobayashi, and K. Asai, J. Phys. Soc. Jpn. **83**, 114712 (2014).
[36] A. Hariki, A. Yamanaka, and T. Uozumi, J. Phys. Soc. Jpn. **84**, 073706 (2015).
[37] R. Suzuki, T. Watanabe, and S. Ishihara, Phys. Rev. B **80**, 054410 (2009).
[38] J. Kunes and V. Krapek, Phys. Rev. Lett. **106**, 256401 (2011).
[39] J. Nasu, T. Watanabe, M. Naka, and S. Ishihara, Phys. Rev. B **93**, 205136 (2016).
[40] M. J. Cooper, P. E. Mijnarends, N. Shiotani, N. Sakai, and A. Bansil, *X-ray Compton Scattering* (Oxford University Press, Oxford, 2004).
[41] A. Koizumi, S. Miyaki, Y. Kakutani, H. Koizumi, N. Hiraoka, K. Makoshi, N. Sakai, K. Hirota, and Y. Murakami, Phys. Rev. Lett. **86**, 5589 (2001).
[42] A. Koizumi, T. Nagao, N. Sakai, K. Hirota, and Y. Murakami, Phys. Rev. B **74**, 012408 (2006).
[43] B. Barbiellini, A. Koizumi, P. E. Mijnarends, W. Al-Sawai, H. Lin, T. Nagao, K. Hirota, M. Itou, Y. Sakurai, and A. Bansil, Phys. Rev. Lett. **102**, 206402 (2009).
[44] Y. Sakurai, M. Itou, B. Barbiellini, P. E. Mijnarends, R. S. Markiewicz, S. Kaprzyk, J.-M. Gillet, S. Wakimoto, M. Fujita, S. Basak, Y. J. Wang, W. Al-Sawai, H. Lin, A. Bansil, and K. Yamada, Science **332**, 698 (2011).
[45] Y. Kobayashi, Y. Sakurai, M. Itoh, K. Sato, and K. Asai, J. Phys. Soc. Jpn. **84**, 114706 (2015).
[46] M. Imada, A. Fujimori, and Y. Tokura, Rev. Mod. Phys. **70**, 1039 (1998).
[47] T. Chiba, J. Chem. Phys. **64**, 1182 (1976).
[48] Note that the calculated Compton profiles and the difference 2D-EMD depicted in Figs. 1 and 2 are not convoluted with the resolution of the Compton scattering measurements.
[49] J. Okamoto, H. Miyauchi, T. Sekine, T. Shidara, T. Koide, K. Amemiya, A. Fujimori, T. Saitoh, A. Tanaka, Y. Takeda, and M. Takano, Phys. Rev. B **62**, 4455 (2000).